Nonstoichiometric Phases of Two-Dimensional Transition-Metal Dichalcogenides: From Chalcogen Vacancies to Pure Metal Membranes

Joseph, T.; Ghorbani Asl, M.; Kvashnin, A. G.; Larionov, K. V.; Popov, Z. I.; Sorokin, P. B.; Krasheninnikov, A.;

Originally published:

October 2019

The Journal of Physical Chemistry Letters 10(2019), 6492-6498

DOI: https://doi.org/10.1021/acs.jpclett.9b02529

Non-Stoichiometric Phases of Two-Dimensional Transition-Metal Dichalcogenides: from Chalcogen Vacancies to Pure Metal Membranes

T. Joseph,[†] M. Ghorbani-Asl,[†] A.G. Kvashnin,[‡] K.V. Larionov,[¶,§] Z. I. Popov,[¶,‖] P.B. Sorokin,[¶,§] and Arkady V. Krasheninnikov[*,†,⊥]

[†]*Institute of Ion Beam Physics and Materials Research, Helmholtz-Zentrum Dresden-Rossendorf, 01328 Dresden, Germany*

[‡]*Skolkovo Institute of Science and Technology, Skolkovo Innovation Center, 3 Nobel Street , Moscow 121205, Russia*

[¶]*National University of Science and Technology "MISIS", Leninsky prospect 4, Moscow 119049, Russia*

[§]*Technological Institute for Superhard and Novel Carbon Materials, 7a Centralnaya Street, Troitsk, Moscow 108840, Russia*

[‖]*Emanuel Institute of Biochemical Physics RAS, Moscow 119334, Russia*

[⊥]*Department of Applied Physics, Aalto University, P.O. Box 11100, 00076 Aalto, Finland*

E-mail: t.joseph@hzdr.de;a.krasheninnikov@hzdr.de

Abstract

Two-dimensional (2D) membranes consisting of a single layer of Mo atoms were recently manufactured [Adv. Mater. 30 (2018) 1707281] from $MoSe_2$ sheets by sputtering Se atoms using electron beam in a transmission electron microscope. This is an unexpected result, as formation of Mo clusters should energetically be more favorable. To get microscopic insights into the energetics of realistic Mo membranes and non-stoichiometric phases of transition metal dichalcogenides (TMDs) M_aX_b, where (M = Mo, W) and (X= S, Se, Te), we carry out first-principles calculations and demonstrate that the membranes, which can be referred to as metallic quantum dots embedded into semiconducting matrix, can be stabilized by charge transfer. We also show that an ideal neutral 2D Mo or W sheet is not flat, but a corrugated structure, with a square lattice being the lowest energy configuration. We further demonstrate that several intermediate non-stoichiometric phases of TMDs are possible, as they have lower formation energies than pure metal membranes. Among them, the orthorhombic metallic 2D M_4X_4 phase is particularly stable. Finally, we study the properties of this phase in detail and discuss how it can be manufactured by the top-down approaches.

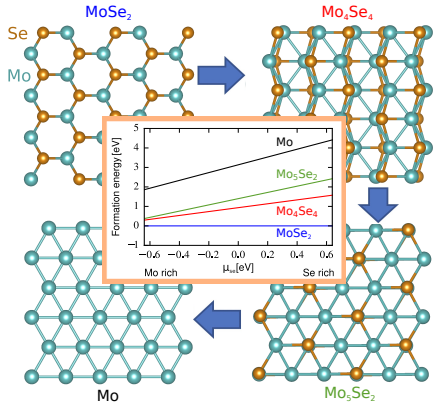

TOC graphic

Recent progress in the mechanical[1] and liquid[2] exfoliation of two-dimensional (2D) systems from layered bulk solids bonded by weak van der Waals (vdW) forces, as well as their direct synthesis by chemical methods,[3] made it possible to manufacture dozens of 2D materials with unique and diverse characteristics. In addition to tailoring their properties for particular applications, the investigations of 2D systems gave rise to a fundamental question: Is it possible to synthesize free-standing 2D counterparts of solids, which normally have bulk isotropic, but not layered, structure? Recent experiments indicated that this is indeed possible, as hematene layers were produced[4] from bulk $\alpha-Fe_2O_3$, which is a non-vdW solid.

Owing to the exotic properties such as highly active surface, charge carries with fast kinetics and surface plasmon resonance, 2D metals offer potential applications for catalyst, battery devices and optical sensors.[5] In that context, lots of attention has also been paid to free-standing 2D metals. Specifically, patches of 2D iron were reported to appear inside graphene nanopores in the transmission electron microscopy (TEM) experiments.[6] Likewise, suspended one-atom-thick Mo membranes were recently fabricated from monolayer $MoSe_2$ sheets via complete sputtering of Se atoms in a scanning TEM.[7] As for the theoretical efforts, the trends in the stability and properties of perfectly flat 2D metals have been studied using first-principles calculations,[8] along with the energetics of small 2D metallic patches embedded in graphene and stabilized by the strong covalent bonds at the metal-graphene interface.[9,10] It should be pointed out, though, that the experimental observations of 2D systems which were interpreted as pure metal membranes could also be explained through the formation of mixed 2D phases, e.g., carbides or oxide, as reported for gold,[11] iron[10,12] or copper,[13] which hints that mixed phases may also be present in case of 2D Mo embedded into $MoSe_2$ sheets.[7]

Specifically, taking into account that Mo sheets were produced by the electron beam by removal of Se atoms from 2D $MoSe_2$, there are several contradictions or points which should be clarified. The membranes were reported to have a hexagonal structure, but the calculated and experimentally measured bond lengths did not match. This may be due to the mechanical strain present in the system, but, as we show below, hexagonal lattice

does not correspond to the lowest energy 2D configuration of Mo. Besides, as Se atoms were gradually (over a time of few minutes) removed by the electron beam, similar to other experiments on the exposure of TMDs to electron-beam irradiation,[14–18] a natural question is why other phases with intermediate stoichiometry were not observed, contrary to, e.g., tin dichalcogenides.[19] This problem is not only of fundamental importance, but it is also directly relevant to the electron-beam engineering of 2D materials.[20–24]

In this work, we use extensive first-principles calculations to study the structure and energetics of 2D metals and non-stoichiometric phases of $MoSe_2$ and some other most common 2D transition metal dichalcogenides (TMDs). The 2D phases were assumed to appear by the formation and aggregation of vacancies in the pristine system. The energetics of the 2D materials with different stoichiometries is analyzed for a wide range of chemical potentials. We further calculate the electronic structure of the most stable non-stoichiometric phase.

Specifically, we employed the density functional theory (DFT) as implemented in the VASP code,[25,26] with the PBE exchange and correlation functional.[27] A plane-wave cut-off of 600 eV was used in all the calculations. The geometry optimization was carried out based on the minimization of the forces acting on the atoms in the structure, with the force tolerance being set to $0.01\,\mathrm{eV\,\AA^{-1}}$. The Brillouin zone of the primitive cells of the materials was sampled with a 12×12×1 Monkhorst-Pack k-mesh. We also carried out test calculations using GPAW code[28] and got similar results.

We simulated both finite metallic patches inside a sheet of the parent TMD and infinite non-stoichiometric sheets assuming that they are also embedded into the 2D TMDs. In the latter case we used two approaches: 'manual' search for the metastable non-stoichiometric phases and 'automatic' search using the USPEX,[29,30] which is a powerful tool for predicting stable compounds of various dimensionalities of given elements. USPEX was successfully extended to 2D materials.[31,32] First the variable-composition search for stable 2D-Mo_xSe_y was performed using the algorithm described in Ref.[33] There were two searches with the initial thickness of the layer equal to 3 and 5 Å, since Mo_xSe_y may prefer non-planar struc-

tures. Both calculations show similar results. There were three the stable structures predicted, namely Mo_5Se_2, MoSe and $MoSe_2$. After that for each stable composition the fixed-composition search was performed in order to predict the most thermodynamically stable structure of each composition. Computational search for free-standing two-dimensional Mo_5Se_2 and MoSe layers were performed with 2, 3, 4, 8 and 12 formula units in the considerd unit cell. The first generation of 160 structures was created using plane group symmetry generator, while all subsequent generations contained 30% random structures, and 80% were created using heredity, softmutation and transmutation variation operators. The newly produced structures were all relaxed, and the energies were used for selecting structures as parents for the new generation of structures. Structure relaxations were performed with the same DFT method with exception that plane wave kinetic energy cutoff was set to 500 eV and the Brillouin zone was samples by Γ-centered k-points meshes with resolution $2\pi \times 0.05^{-1}$. Phonon density of states of predicted MoSe was calculated using finite displacement method as implemented in the PHONOPY code.[34]

The annular dark field scanning TEM (ADF-STEM) image simulations were carried out with the Dr. Probe[35] code assuming an aberration-free probe and 5 Å source size to give a focus spread of 3.0 nm. The STEM simulations were performed at 80 kV with 30 mrad illumination half angle and 20 mrad outer detection angle.

We studied first the energetics of the periodic 2D phases of transition metals, which are present in the most common TMDs: Mo and W. To assess the stability of 2D metals, the atomic structure of various 2D infinite periodic systems was fully optimized without any constraints, and cohesive energy E_{cohesive} was calculated. It was defined as usual as $E_{\text{cohesive}} = E_{\text{atom}} - \frac{E(N)}{N}$, where E_{atom} is the energy of an isolated atom, E is the energy of the structure and N the total number of atoms in the unit cell. Note that E_{cohesive} is positive, and larger values indicate a higher stability of the system.

The atomic structures of transition metal membranes and the associated cohesive energies are presented in Fig.1. Contrary to the simulation setup employed in Ref.,[8] where perfectly

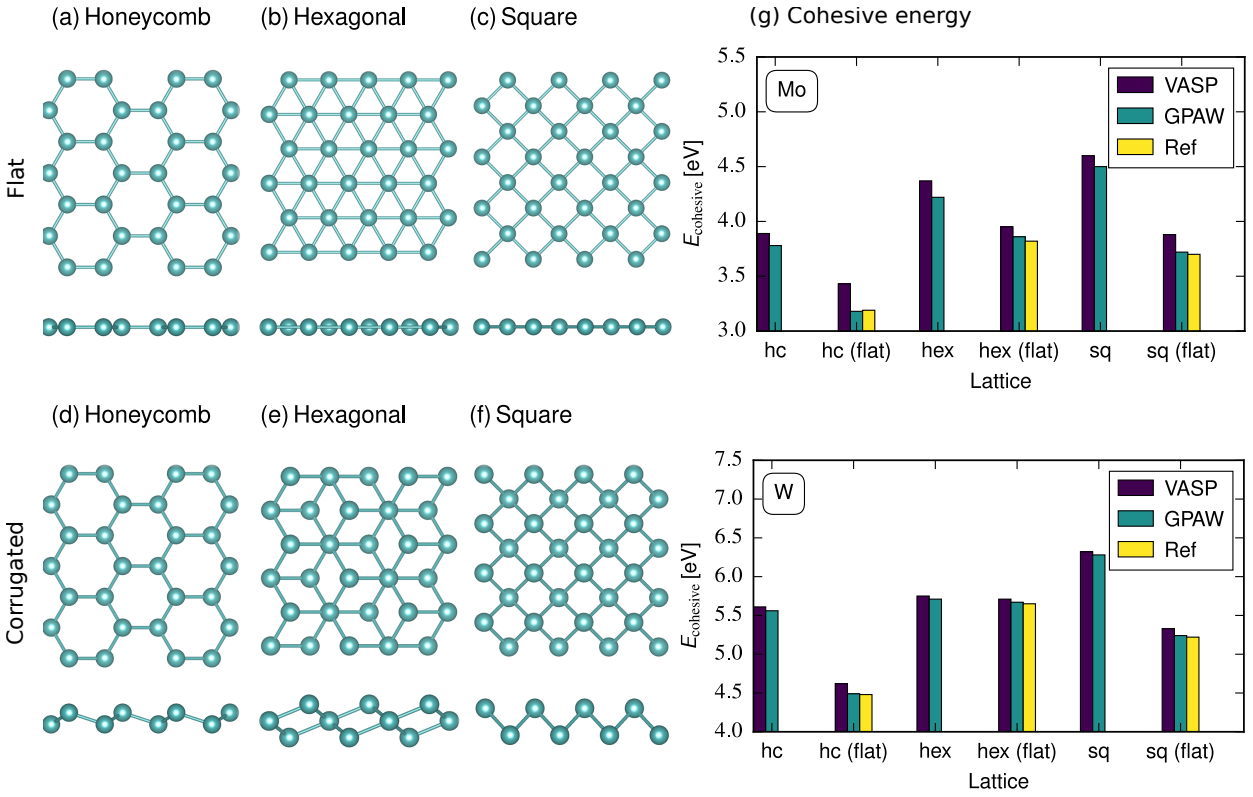

Figure 1: Atomic structures of 2D phases of Mo and W, top and side views, for the constrained (flat) atomic network, panels (a-c), and those obtained without any constraints (d-f). (g) Comparison of cohesive energy of 2D phase of Mo and W as calculated using VASP and GPAW codes. The data represented by yellow bars are taken from Ref.[8]

flat structures were studied to get insights into the trends in the geometry and bonding, we allowed out-of-plane relaxation. Our results for flat structures proved to be in a good agreement with those presented in Ref.,[8] and the hexagonal (flat) phase was found to have the highest cohesive energy for both Mo and W. However, our simulations indicate that when out-of-plane relaxation is allowed, the most energetically favorable phase is the square one. This stresses the importance of the out-of-plane degrees of freedom for the realistic 2D materials in the three-dimensional space.

However, Mo hexagonal lattice was observed in the experiment,[7] contrary to the most energetically favorable square lattice. The experimental bond length was found to be 2.7 Å. From our simulations, the apparent separation between the atoms (projected into the plane) in the corrugated hexagonal lattice and planar hexagonal lattice is 2.47 Å and 2.57 Å respec-

tively in case of Mo. Because the Mo domains are formed by sputtering of Se atoms from $MoSe_2$, the islands may be subjected to tensile strain, but to match the experiment, strain must be rather high, nearly 10%. Moreover, careful analysis of the TEM images shown in Figs. 1-3 in Ref.[7] using the scale bar of 5 Å indicates that many bonds are much longer, nearly 3 Å. The same conclusion also can be drawn from the analysis of atomically perfect grain boundary between $MoSe_2$ and new phase which suggests close lattice constants of both phases. The tensile strain of 20% is unrealistically high, especially with account for migration of Mo atoms into the membrane areas, as observed in the experiment,[7] and in general it is unclear why hexagonal lattice is preferred.

To understand the reason for large separations between the atoms, we considered possible charging of Mo membranes. A Mo island in $MoSe_2$ sheet is essentially a quantum dot embedded into a semiconductor matrix. If the sample is n-type doped, it may give rise to negative charge accumulation. The additional charge may also come from other defects created in $MoSe_2$ by the electron beam[36–38] or adsorption of impurities[39] on these defects, which gives rise to the occupied or partially occupied defect-induced states in the gap.

Simulations for the neutral and charged systems were conducted and the results are presented in Fig. 2. In the neutral system considered, a small cluster of metal atoms is formed, and the cluster moves then to one of the edges. The behavior of the charged system is different. As evident from Fig. 2(c), the extra charge is localized in the membrane area, giving rise to longer bonds between the metal atoms. From the radial distribution function shown in Fig. 2(d) it is clear that charging of the system improves the agreement between theory and experiment.[7] With a charge of $0.2\,e$, the bond length of the structure matches well the experimental value of 2.7 Å with some distortions at the edges at the interface to $MoSe_2$. Moreover, calculations for infinite free-standing metals showed that the hexagonal phase is energetically preferable over square lattice when an additional charge is added.

As an alternative scenario, we also investigated the changes in the atomic structure of the membrane when extra Mo atoms are added to the system, Fig. 2(b). Extra atoms do

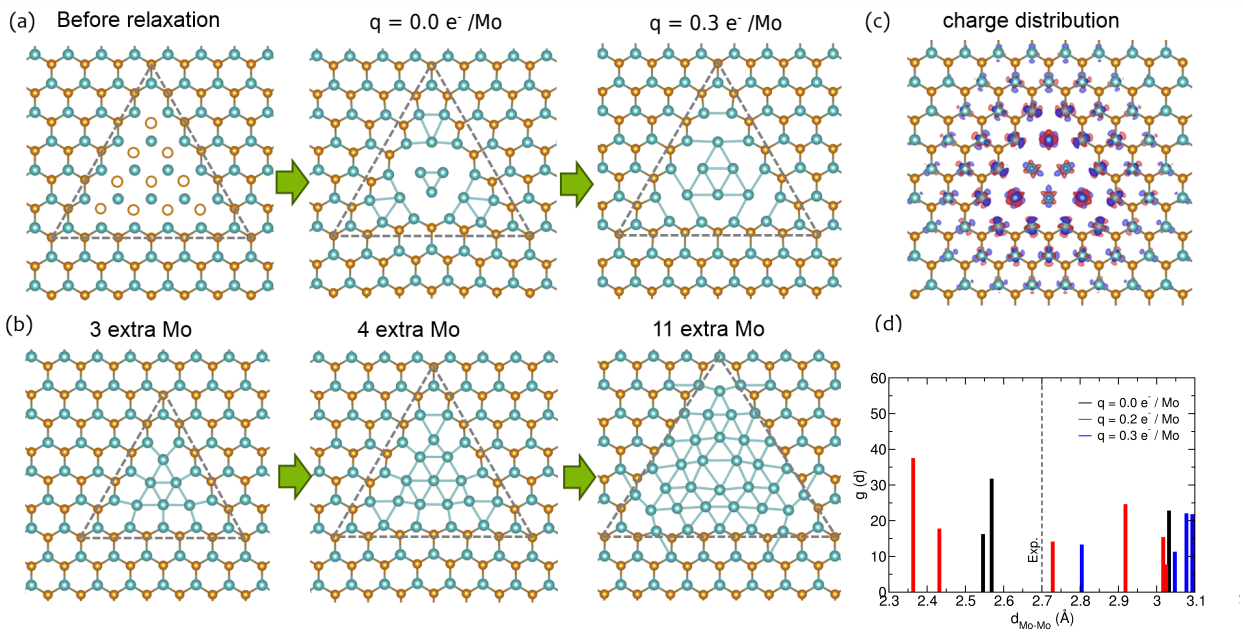

Figure 2: (a) Illustration of the evolution of the atomic structure of the metal membrane upon introduction of additional charge. It is evident that extra charge increases inter-atomic distances. (b) Optimized structure of the membrane with extra Mo atoms. (c) Charge density distribution with extra $0.3\,e$ charge in the system. (d) Radial distribution function for the neutral and charged system.

stabilize the membrane, but interatomic distances are smaller than in the experiment, as clear from Fig. 2(b) and the analysis of the radial distribution function. Based on these results, it appears that accumulation of the extra charge is the main reason for the stabilization of the membrane and rather a long separation between the Mo atoms.

As in the experiment Se atoms were gradually (over a time of few minutes) sputtered by the electron beam before patches of pure metals were produced, we also studied phases with intermediate stoichiometry, which hypothetically can also appear in the chalcogen-deficient material. We considered various non-stoichiometric binary compounds $M_yX_{2(1-y)}$, where M = Mo, W and X= S, Se, Te. Mimicking the experimental situation, the phases were created by adding vacancies to the pristine structure and optimizing the geometry. Some of the structures we studied are shown in Fig.3. The stability of these phases, which should naturally depend on the chemical potentials of the atoms was evaluated by calculating the formation energies of the structures. Assuming that the non-stoichiometric phase is

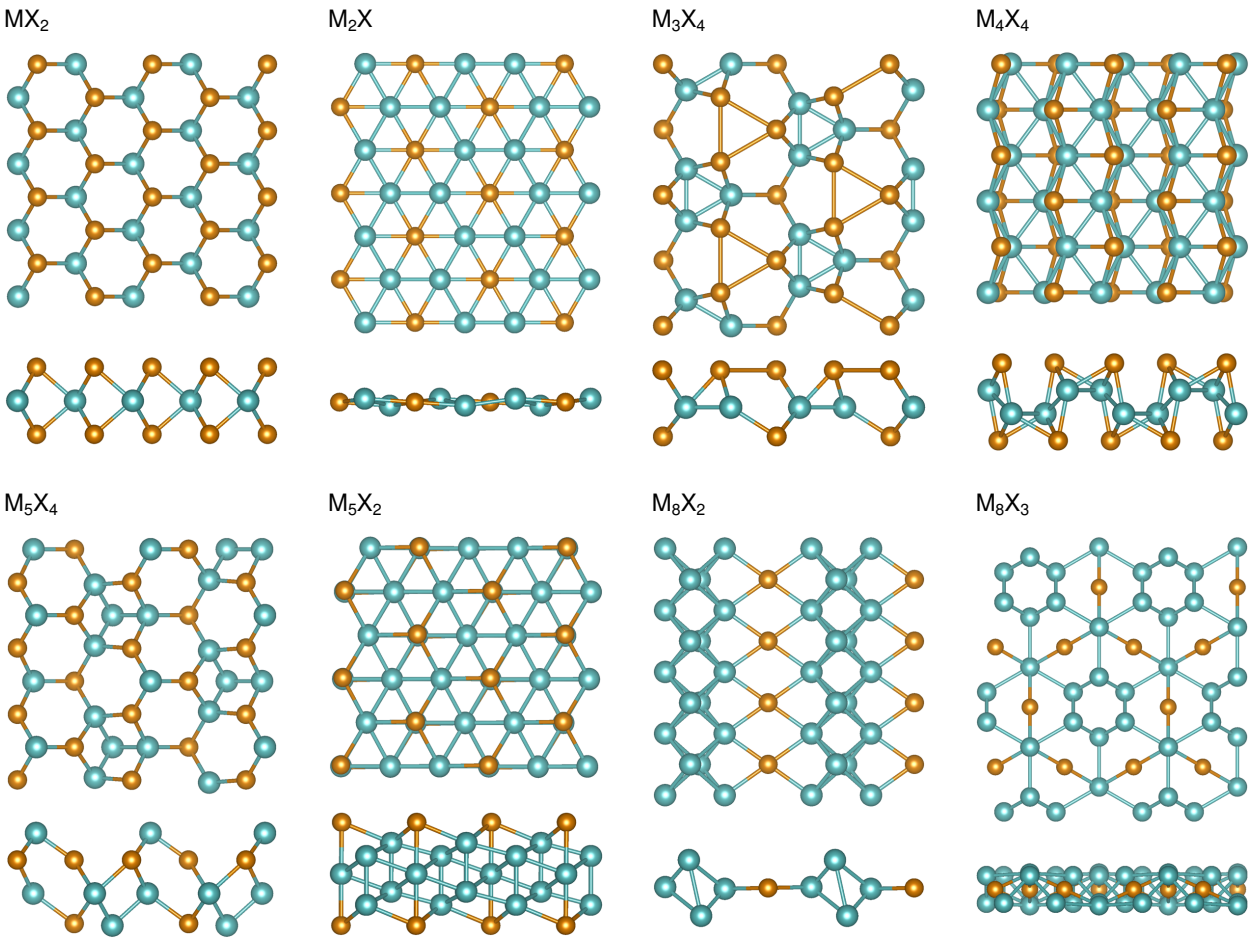

Figure 3: Atomic structures of non-stoichiometric phases of binary compounds formed from transition metal (M, M = Mo, W) and chalcogen (X, X= S, Se, Te) atoms, top and side views.

embedded into the pristine stoichiometric phase, the energetics (formation energy E_f per formula unit) of the phase M_aX_b consisting of a transition metal atoms and b chalcogen atoms, was calculated as a function of chalcogen atom chemical potential μ_X as:

$$E_{\rm f} = \frac{E(\mathrm{M_aX_b})}{a} - E(\mathrm{MX_2}) + \frac{2a-b}{a}\mu_{\rm X}, \tag{1}$$

where $E(\mathrm{M_aX_b})$ and $E(\mathrm{MX_2})$ are the total energies of the primitive cells of the non-stoichiometric and stoichiometric phases respectively. Correspondingly, for any value of $\mu_{\rm X}$ formation energy $E_{\rm f}$ of the $\mathrm{MX_2}$ phase is zero. Equation (1) is essentially the formation energy of a defect

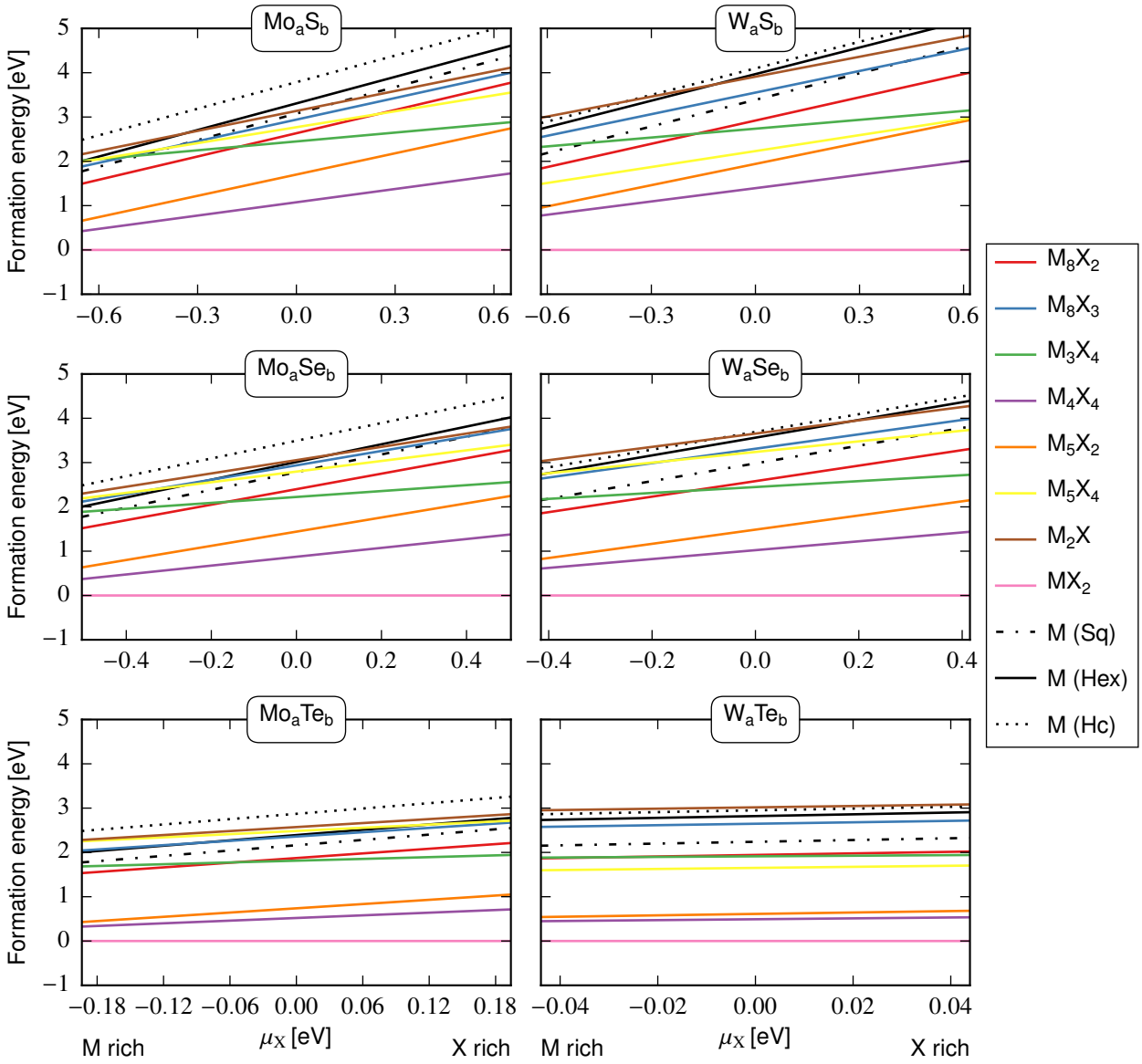

Figure 4: Formation energies of non-stoichiometric phases and pure metal membranes embedded into pristine material as functions of chalcogen atom chemical potentials.

in the pristine material normalized to the defect area. We stress that in these calculations we do not take into account the actual structure of the interface between the stoichiometric and non-stoichiometric phases, assuming that the structure is large enough, so that the interfaces can be neglected. It can also be used to assess the energy loss for removing all chalcogen atoms from the system and forming a pure metal membrane. As the phase is embedded into

the stoichiometric phase, it is assumed that for any stoichiometry:

$$\mu_{\mathrm{M}} + 2\mu_{\mathrm{X}} = \mu_{\mathrm{MX}_2}, \tag{2}$$

where the value of μ_{M} and μ_{X} are limited by the lowest energy phases.

The formation energies for non-stoichiometric phases and for pure metal membranes are shown in Fig.4. It is seen that there are non-stoichiometric phases that are more stable than pure 2D metals. The most stable non-stoichiometric phase from the simulation is M_4X_4, with the energy difference between the hexagonal metal phase and M_4X_4 being over 1 eV. As evident from Fig.4, the energy difference between this and the stoichiometric phase is 0.3-0.6 eV in the metal-rich limit, which indicates that the phase can potentially be synthesized or manufactured using electron beam by sputtering chalcogen atoms, e.g. by using moderate heating during irradiation. Another non-stoichiometric phase of interest is M_5X_2, which, unlike M_4X_4, has a hexagonal lattice with a formation energy comparable to the lowest energy M_4X_4 at the metal-rich end. The phase can be referred to as a corrugated Mo sheet with attached chalcogen atoms, and it is a likely candidate for forming domains when chalcogen atoms are sputtered away by the electron beam.

Although we considered single-layer structures, the van der Waals (vdW) interaction is known to affect the cohesive energies of non-layered materials by up to 0.3 eV per atom, especially when defects are present [for an overview, see [40]]. To address this issue, we repeated the calculations of the total energies and geometries of all the phases of the MoSe system we considered with the Tkatchenko-Scheffler vdW exchange and correlation functional.[41] The primitive cell size of every phase was carefully optimized. The account for the vdW interaction decreased the energy difference between the non- stoichiometric phases and MoSe by 0.1–0.3 eV, but did not change the qualitative picture. The geometry of the systems remained the same and the Mo membrane was still corrugated.

To further facilitate a comparison with the experimental results,[7] we simulated STEM

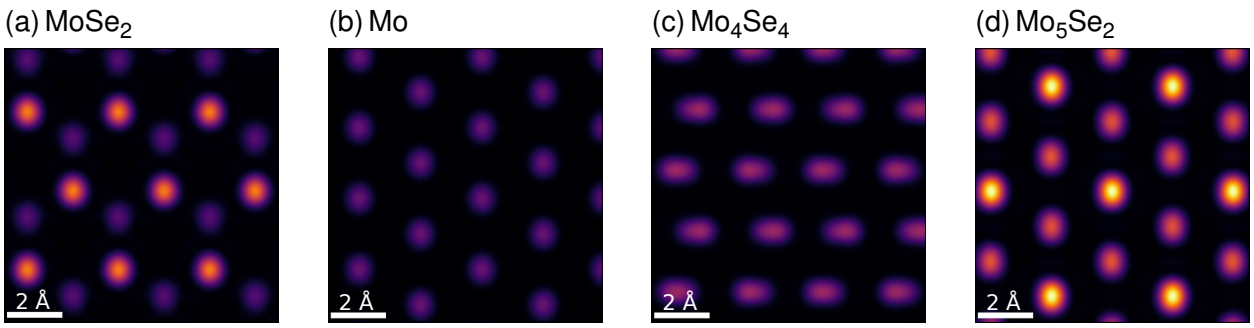

Figure 5: Simulated annular dark field scanning transmission electron microscopy images of the Mo_4Se_4 and Mo_5Se_2 phases in comparison to pure Mo membrane and $MoSe_2$ at 80 kV. The intensity scale is the same for all the images.

images of the phases with the lowest energies, along with those for pure Mo membrane and pristine $MoSe_2$. Fig.5 presents the simulated STEM images of the Mo_4Se_4 and Mo_5Se_2 phases in comparison to pure Mo membrane and $MoSe_2$. The intensity scale is the same for all the images. Interestingly the Mo_5Se_2 has a slightly distorted hexagonal lattice with a lattice constant of ≈ 2.7 Å, close to the experimental result reported in Ref.[7] On the other hand, the simulated metallic Mo membrane has a lattice constant of only 2.57 Å. Thus some areas in the irradiated $MoSe_2$ sheets maybe not purely metallic phase, but one of the mixed phases.

Independently, we also carried out a global minimum search of non-stochiometric 2D structures by the evolutionary algorithm. The simulation yielded the same 2D molybdenum monoselenide with distorted puckered honeycomb lattice of orthorhombic symmetry, Fig.4(d) and Fig.5(c). Such phase has lattice parameters $a = 5.455$ Å, $b = 4.449$ Å($Pbcm$ space group) with one Mo atom (0.402, 0.250, 0.477) and one Se atom (-0.016, 0.250, 0.425). Dynamical stability of predicted monolayer was studied by the phonon calculations, shown in Fig.6. One can see no imaginary phonon modes, Fig. Fig.6(a), so that even the free-standing structure should be stable. Presence of a substrate will further stabilize this phase. The elastic constants of the Mo_4Se_4 phase were found to be $C_{11} = 87.1$ N/m, $C_{22} = 204.7$ N/m, $C_{12} = 46.4$ N/m, $C_{66} = 53.7$ N/m. One elastic constant of uniaxial deformation (C_{22}) is almost two times larger than the corresponding value for $MoSe_2$ (110.5 N/m) whereas another constant (C_{11}) is slightly lower.

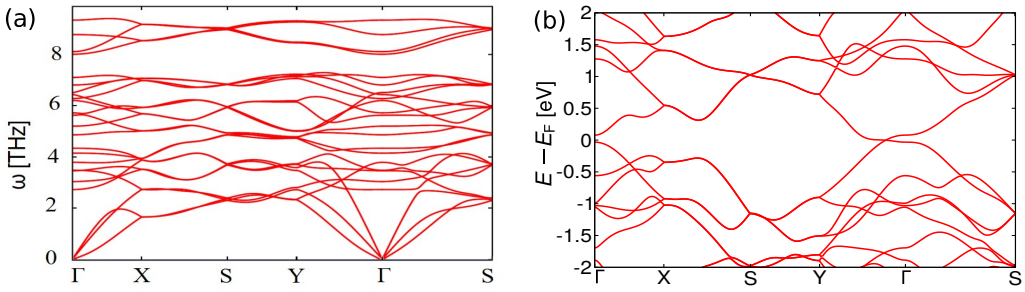

Figure 6: (a) Phonon dispersion and (b) electronic structure of Mo_4Se_4 phase.

We further calculated the electronic structure of the Mo_4Se_4 phase. The PBE band structure of Mo_4Se_4 is shown in Fig.6(b). It is evident that the phase is metallic. We obtained similar results for other M_4X_4 systems. The metallic nature of these compounds was also confirmed by the G_0W_0 calculations.

To sum up, using first-principles calculations we demonstrated that the lowest energy configuration of a neutral 2D membrane composed from Mo atoms only is not the hexagonal, as previously assumed,[8] but the square lattice. The structure is not flat, but develops out-of-plane corrugation. However, when a finite-size Mo membrane embedded into a semiconducting $MoSe_2$ material is negatively charged, the lowest energy configuration corresponds to the hexagonal lattice, which has experimentally been observed,[7] provided that indeed no other chemical element (e.g., carbon, oxygen) is present, as confirmed by EELS. We further showed that the extra charge also gives rise to increased separations between the atoms, which may explain the apparent contradiction between the bond lengths obtained in the calculations and those experimentally measured in Mo membranes derived from $MoSe_2$ sheets by sputtering Se atoms using the electron beam in the scanning TEM.[7] We also provide evidence that other non-stoichiometric 2D phases of $MoSe_2$ and other TMDs MX_2(M=Mo, W; X = S, Se, Te) with low formation energies can exist. Among these 2D phases, the 2D M_4X_4 and M_5X_2 phases are particularly stable, especially in the Mo-rich limit, which corresponds to the conditions in the TEM experiments. This indicates that although the formation of the pure Mo/W phase may be related to the dynamical effects and preferential sputtering of chalcogen atoms, it should in principle be possible to quench the system into

this configuration by, e.g., moderate heating of the sample during exposure to the electron beam. The lowest energy M_4X_4 phase is metallic, contrary to the original material, which is a semiconductor. This potentially opens new avenues for patterning and atomic-scale engineering of the properties of 2D TMDs with high miniaturization and integration. As exposure to chalcogen atoms combined with annealing will likely lead to the restoration of the original structure, the system can be used in rewritable electronics.

Acknowledgements. We thank J. Nevalaita and P. Koskinen for discussions. We acknowledge funding from the German Research Foundation (DFG), projects KR 48661/1 and KR 48661/2, and the Academy of Finland under Project No. 286279. We also acknowledge the financial support of the Ministry of Education and Science of the Russian Federation in the framework of Increase Competitiveness Program of NUST "MISiS" (No. K2-2019-016) and Grant of President of Russian Federation for government support of young DSc. (MD-1046.2019.2). Study of Mo_4Se_4 monolayer was supported by Russian Science Foundation (Project identifier: 17-72-20223). The further thank CSC Finland, PRACE (HLRS, Stuttgart, Germany) and TUD (Taurus cluster) for generous grants of CPU time.

References

(1) Radisavljevic, B.; Radenovic, A.; Brivio, J.; Giacometti, V.; Kis, A. Single-layer MoS2 transistors. Nature Nanotech. **2011**, 6, 147–50.

(2) Coleman, J. N.; Lotya, M.; Neill, A. O.; Bergin, S. D.; King, P. J.; Khan, U.; Young, K.; Gaucher, A.; De, S.; Smith, R. J. et al. ïż£Two-dimensional nanosheets produced by Liquid Exfoliation of Layered Materials. Science **2011**, 331, 568–571.

(3) Zhan, Y.; Liu, Z.; Najmaei, S.; Ajayan, P. M.; Lou, J. Large-Area Vapor-Phase Growth and Characterization of MoS_2 Atomic Layers on a SiO_2 Substrate. Small **2012**, 8, 966–971.

(4) Puthirath Balan, A.; Radhakrishnan, S.; Woellner, C. F.; Sinha, S. K.; Deng, L.; Reyes, C. D. L.; Rao, B. M.; Paulose, M.; Neupane, R.; Apte, A. et al. Exfoliation of a non-van der Waals material from iron ore hematite. Nature Nanotech. **2018**, 13, 602–609.

(5) Ma, Y.; Li, B.; Yang, S. Ultrathin two-dimensional metallic nanomaterials. Mater. Chem. Front. **2018**, 2, 456–467.

(6) Zhao, J.; Deng, Q.; Bachmatiuk, A.; Sandeep, G.; Popov, A.; Eckert, J.; Rümmeli, M. H. Free-Standing Single-Atom-Thick Iron Membranes Suspended in Graphene Pores. Science **2014**, 343, 1228–1232.

(7) Zhao, X.; Dan, J.; Chen, J.; Ding, Z.; Zhou, W.; Loh, K. P.; Pennycook, S. J. Atom-by-Atom Fabrication of Monolayer Molybdenum Membranes. Adv. Mater. **2018**, 30, 1707281.

(8) Nevalaita, J.; Koskinen, P. Atlas for the properties of elemental two-dimensional metals. Phys. Rev. B **2018**, 97, 035411.

(9) Chen, S.; Zeng, X. C. Interaction between Iron and Graphene Nanocavity: Formation of Iron Membranes, Iron Clusters, or Iron Carbides. ACS Applied Materials and Interfaces **2017**, 9, 12100–12108.

(10) Larionov, K. V.; Kvashnin, D. G.; Sorokin, P. B. 2D FeO: A New Member in 2D Metal Oxide Family. J. Phys. Chem. C **2018**, 122, 17389–17394.

(11) Westenfelder, B.; Biskupek, J.; Meyer, J. C.; Kurasch, S.; Lin, X.; Scholz, F.; Gross, A.; Kaiser, U. Bottom-up formation of robust gold carbide. Scientific Reports **2015**, 5, 8891.

(12) Shao, Y.; Pang, R.; Shi, X. Stability of Two-Dimensional Iron Carbides Suspended across Graphene Pores: First-Principles Particle Swarm Optimization. J. Phys. Chem. C **2015**, 119, 22954–22960.

(13) Kano, E.; Kvashnin, D. G.; Sakai, S.; Chernozatonskii, L. A.; Sorokin, P. B.; Hashimoto, A.; Takeguchi, M. One-atom-thick 2D copper oxide clusters on graphene. Nanoscale **2017**, 9, 3980–3985.

(14) Zhou, W.; Zou, X.; Najmaei, S.; Liu, Z.; Shi, Y.; Kong, J.; Lou, J.; Ajayan, P. M.; Yakobson, B. I.; Idrobo, J.-C. Intrinsic Structural Defects in Monolayer Molybdenum Disulfide. Nano Lett. **2013**, 13, 2615–2622.

(15) Parkin, W. M.; Balan, A.; Liang, L.; Das, P. M.; Lamparski, M.; Naylor, C. H.; Rodríguez-Manzo, J. A.; Johnson, A. T.; Meunier, V.; Drndić, M. Raman Shifts in Electron-Irradiated Monolayer MoS2. ACS Nano **2016**, 10, 4134–4142.

(16) Lehnert, T.; Ghorbani-Asl, M.; Köster, J.; Lee, Z.; Krasheninnikov, A. V.; Kaiser, U. Electron-Beam-Driven Structure Evolution of Single-Layer MoTe 2 for Quantum Devices. ACS Appl. Nano Mater. **2019**, 2, 3262–3270.

(17) Lin, J.; Pantelides, S. T.; Zhou, W. Vacancy-Induced Formation and Growth of Inversion Domains in Transition-Metal Dichalcogenide Monolayer. ACS Nano **2015**, 9, 5189–5197.

(18) Wang, S.; Lee, G.-D.; Lee, S.; Yoon, E.; Warner, J. Detailed Atomic Reconstruction of Extended Line Defects in Monolayer MoS 2. ACS Nano **2016**, 10, 5419–5430.

(19) Sutter, E.; Huang, Y.; Komsa, H.-P.; Ghorbani-Asl, M.; Krasheninnikov, A. V.; Sutter, P. Electron-Beam Induced Transformations of Layered Tin Dichalcogenides. Nano Lett. **2016**, 16, 4410–4416.

(20) Krasheninnikov, A. V.; Banhart, F. Engineering of Nanostructured Carbon Materials with Electron or Ion Beams. Nat. Mater. **2007**, 6, 723–733.

(21) Kalinin, S. V.; Borisevich, A.; Jesse, S. Fire up the atom forge. Nature **2016**, 539, 485–487.

(22) Lin, Z.; Carvalho, B. R.; Kahn, E.; Lv, R.; Rao, R.; Terrones, H.; Pimenta, M. A.; Terrones, M. Defect Engineering of Two-Dimensional Transition Metal Dichalcogenides. 2D Mater. **2016**, 3, 022002.

(23) Krasheninnikov, A. V.; Nordlund, K. Ion and Electron Irradiation-Induced Effects in Nanostructured Materials. J. Appl. Phys. **2010**, 107, 071301.

(24) Zhao, X.; Kotakoski, J.; Meyer, J. C.; Sutter, E.; Sutter, P.; Krasheninnikov, A. V.; Kaiser, U.; Zhou, W. Engineering and modifying two-dimensional materials by electron beams. MRS Bulletin **2017**, 42, 667–676.

(25) Kresse, G.; Furthmüller, J. Comp. Mat. Sci. **1996**, 6, 15.

(26) Kresse, G.; Furthmüller, J. Efficient iterative schemes for ab initio total-energy calculations using a plane-wave basis set. Phys. Rev. B **1996**, 54, 11169–11186.

(27) Perdew, J. P.; Burke, K.; Ernzerhof, M. Generalized Gradient Approximation Made Simple. Phys. Rev. Lett. **1996**, 77, 3865–3868.

(28) Enkovaara, J.; Rostgaard, C.; Mortensen, J. J.; Chen, J.; Dułak, M.; Ferrighi, L.; Gavnholt, J.; Glinsvad, C.; Haikola, V.; Hansen, H. A. et al. Electronic structure calculations with GPAW: a real-space implementation of the projector augmented-wave method. J. Phys. Condens. Matter **2010**, 22, 253202.

(29) Oganov, A. R.; Glass, C. W. Crystal structure prediction using ab initio evolutionary techniques: Principles and applications. J. Chem. Phys. **2006**, 124, 244704.

(30) Lyakhov, A. O.; Oganov, A. R.; Stokes, H. T.; Zhu, Q. New developments in evolutionary structure prediction algorithm USPEX. Computer Physics Communications **2013**, 184, 1172 – 1182.

(31) Zhou, X.-F.; Dong, X.; Oganov, A. R.; Zhu, Q.; Tian, Y.; Wang, H.-T. Semimetallic Two-Dimensional Boron Allotrope with Massless Dirac Fermions. Phys. Rev. Lett. **2014**, 112, 085502.

(32) Wang, Z.; Zhou, X.-F.; Zhang, X.; Zhu, Q.; Dong, H.; Zhao, M.; Oganov, A. R. Phagraphene: A Low-Energy Graphene Allotrope Composed of 5-6-7 Carbon Rings with Distorted Dirac Cones. Nano Lett. **2015**, 15, 6182–6186.

(33) Revard, B. C.; Tipton, W. W.; Yesypenko, A.; Hennig, R. G. Grand-canonical evolutionary algorithm for the prediction of two-dimensional materials. Phys. Rev. B **2016**, 93, 054117.

(34) Togo, A.; Tanaka, I. First principles phonon calculations in materials science. Scripta Materialia **2015**, 108, 1 – 5.

(35) Barthel, J. Dr. Probe: A software for high-resolution STEM image simulation. Ultramicroscopy **2018**, 193, 1–11.

(36) Shafqat, A.; Iqbal, T.; Majid, A. A DFT study of intrinsic point defects in monolayer MoSe2. AIP Advances **2017**, 7, 105306.

(37) Lehtinen, O.; Komsa, H. P.; Pulkin, A.; Whitwick, M. B.; Chen, M. W.; Lehnert, T.; Mohn, M. J.; Yazyev, O. V.; Kis, A.; Kaiser, U. et al. Atomic scale microstructure and properties of se-deficient two-dimensional MoSe2. ACS Nano **2015**, 9, 3274–3283.

(38) Komsa, H.-P.; Krasheninnikov, A. V. Engineering the Electronic Properties of Two-Dimensional Transition Metal Dichalcogenides by Introducing Mirror Twin Boundaries. Adv. El. Mater. **2017**, 3, 1600468.

(39) Guo, Y.; Ji, Y.; Dong, H.; Wang, L.; Li, Y. Electronic and optical properties of defective MoSe2 repaired by halogen atoms from first-principles study. AIP Advances **2019**, 9, 025202.

(40) Tkatchenko, A. Current Understanding of Van der Waals Effects in Realistic Materials. Adv. Func. Mater. **2015**, 25, 2054–2061.

(41) Tkatchenko, A.; Scheffler, M. Accurate Molecular Van Der Waals Interactions from Ground-State Electron Density and Free-Atom Reference Data. Phys. Rev. Lett. **2009**, 102, 073005.